DOI: 10.1002/chem.200901715

Synthesis of Enantiopure Sulfonimidamides and Elucidation of Their Absolute Configuration by Comparison of Measured and Calculated CD Spectra and X-Ray Crystal Structure Determination

Christin Worch, Iuliana Atodiresei, Gerhard Raabe, and Carsten Bolm*[a]

Abstract: Straightforward syntheses of enantiopure *N*-benzoyl- and *N*-*tert*-butyloxycarbonyl-protected sulfonimidamides, which can be used as building blocks in newly designed catalysts, are presented. Key synthetic step is a dynamic resolution of a racemic sulfinic acid sodium salt. All subsequent transformations proceed stereospecifically. The absolute configurations at the sulfur atoms of both sulfonimidamides were determined by comparison of measured and calculated CD spectra. An X-ray crystal structure determination of a sulfonimidoylguanidine derivative confirmed this result.

Keywords: absolute configuration · circular dichroism · resolution · sulfonimidamide

Introduction

Sulfonimidamides have recently been applied as nitrene sources in rhodium-catalyzed C–H aminations,[1] metal-catalyzed olefin aziridinations[2] and preparation of sulfimides and sulfoximines.[2a,3] Coupling reactions of sulfonimidamides with uronium reagents yielded sulfonimidoylguanidines,[4] and *N*-arylated derivatives were obtained by copper-mediated C–N bond formation.[5] Mitsunobu reactions involving the free amino group afforded *N*-heterocycles.[6–8]

In most of the reactions described the sulfonimidamides were used as racemates. Only a few enantiopure sulfonimidamides are known and most of them have *N*-methyl, *N*-tosyl or *N*-nosyl groups.[1,2c,3,7] Herein we report the synthesis of *N*-benzoyl- (*N*-Bz) and *N*-*tert*-butyloxycarbonyl- (*N*-Boc) protected sulfonimidamides and the determination of their absolute configuration by comparison of calculated and measured CD spectra.

Results and Discussion

As outlined in Scheme 1, the *N*-protected enantiopure sulfonimidamides could readily be prepared by a four-step reaction sequence: First, commercially available racemic 4-toluenesulfinic acid sodium salt (**1**) was converted into menthyl ester **2** via the corresponding sulfinic acid chloride.[9] An epimerization shifted the equilibrium of the diastereomers and allowed sulfinate ester **2** to be obtained with >99% de in up to 70% yield after recrystallization. Next, ester **2** was reacted with lithium hexamethyldisilazide (LiHMDS) forming a bis(trimethylsilylamide) which upon hydrolysis gave (*S*)-sulfinamide **3** with >99% *ee* in 87% yield after recrystallization.[10] For the preparation of *N*-acylsulfinamides **4** or **5**, sulfinamide **3** was treated with 2.5 equiv of *n*-butyl lithium followed by the addition of di-*tert*-butyl dicarbonate or benzoic acid anhydride, respectively.[11] The *N*-substituted sulfinamides **4** and **5** were obtained in good yields with complete retention of configuration. Subsequent oxidative chlorination using *tert*-butyl hypochlorite[12–14] and treatment of the resulting (*R*)-sulfonimidoyl chlorides **6** and **7** with an aqueous solution of ammonia afforded *N*-substituted sulfonimidamides **8** and **9** with >99% *ee* in 78 and 97% yield, respectively.

The findings of Johnson[7d] and Reggelin[13] on related systems suggested that the nucleophilic chloride displacement of sulfonimidoyl chlorides **6** and **7** with ammonia occurred with inversion of configuration. In order to confirm this hypothesis and to ensure the stereochemistry of the products it was decided to determine their absolute configuration by experimental and theoretical CD spectroscopy, which allowed establishing the spatial arrangement of the substituents at the chiral sulfur atom with a high degree of probability.

[a] C. Worch, Dr. I. Atodiresei, Prof. Dr. G. Raabe, Prof. Dr. C. Bolm
Institute of Organic Chemistry, RWTH Aachen University
Landoltweg 1, 52056 Aachen (Germany)
Fax: (+49) 241-8092391
E-mail: carsten.bolm@oc.rwth-aachen.de

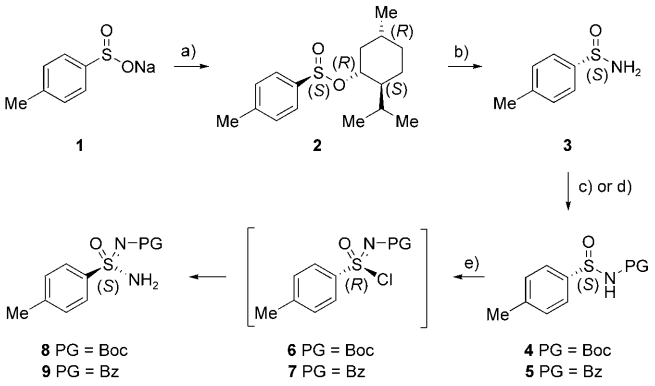

Scheme 1. Synthesis of the sulfonimidamides **8** and **9**: a) $SOCl_2$ (1.2 equiv), Et_2O (0.6 mmol mL^{-1}), 0 °C → RT, 2 h; then L-menthol (1.1 equiv), pyridine (1.5 equiv), Et_2O (1.0 mmol mL^{-1}), RT, overnight; recrystallization from acetone, 70%; b) LiHMDS (1.06 M in THF, 1.5 equiv), THF (0.2 mmol mL^{-1}), −78 °C → RT, 2 h; then sat. aq. NH_4Cl (2.5 mL pro mmol of **2**), RT, 1.5 h, 87%; c) *n*-butyl lithium (1.6 M in hexane, 2.5 equiv), Boc_2O (1.2 equiv), THF (0.8 mmol mL^{-1}), −78 → 0 °C, 3 h, 63% d) *n*-butyl lithium (1.6 M in hexane, 2.5 equiv), Bz_2O (1.2 equiv), THF (0.2 mmol mL^{-1}), −78 → 0 °C, 3 h, 61%; e) *tert*-butyl hypochlorite (1.3 equiv), THF (0.06-0.13 mmol mL^{-1}), 0 °C, 2 h; then NH_3 (25% in H_2O, 4 mL pro mmol of **4** or **5**), RT, overnight, 78% for **8** and 97% for **9**.

Computational Details

A Monte-Carlo conformational search[15] using the program Spartan '02[16] with default parameters and convergence criteria and the MMFF[17] provided initial sets of geometries for sulfonimidamides **8** and **9**. The subsequent ab initio geometry optimizations were performed for isolated molecules in the gas phase using a medium size basis set (6-31+G*) and including correlation energy by means of second-order Møller-Plesset perturbation theory as implemented in the program Gaussian 03.[18] Starting with the arbitrarily chosen *R* enantiomer, 11 and 5 stationary points were located at the MP2/6-31+G* level for **8** and **9**, respectively. Additional single point energy calculations were then performed at the MP2/6-311++G**//MP2/6-31+G* level, and the final energies were corrected with the unscaled zero-point energy (ZPE) calculated at the MP2/6-31G* level. The relative energies as well as the geometries of the six most stable conformers of **8** (E_{rel} < 2.5 kcal mol^{-1}) and all conformers of **9** are presented in Tables 1 and 2, respectively.[19]

Theoretical CD spectra were obtained using the time-dependent density functional theory (TDDFT)[20] employing the B3LYP functional[21] and a valence triple zeta basis set, including polarization and diffuse functions (6-311++G**). The rotational strengths have been calculated using the origin-independent dipole-velocity formalism.[22] The CD curve ($\Delta\varepsilon_i$) of each conformer *i* was represented as a sum of Gaussian curves. Each of the Gaussians is centered at the calculated wavelength of the corresponding transition and multiplied with its rotational strength.[23] The half bandwidth Γ at $\Delta\varepsilon_{max}$/e was obtained using the empirical formula $\Gamma = k\cdot\lambda^{1.5}$ where λ is the transition wavelength and *k* an empirical parameter.[24] In our study we used a value of $k = 0.00375$[25] yielding half bandwidths covering the range from 6.9 to 30.0 between 150 and 400 nm. The final CD curve ($\Delta\varepsilon$) was generated by Boltzmann-weighted superposition of the N CD spectra of the single conformers. The Boltzmann factors (298 K) were calculated by using the ZPE+MP2/6-311++G**//MP2/6-31+G* relative energies.

Table 1. Structures of the six most stable conformers of (*R*)-**8** (**8a–f**) optimized at the MP2/6-31+G* level and their total (in Hartrees) and relative energies (in kcal mol^{-1}) including the ZPE correction.

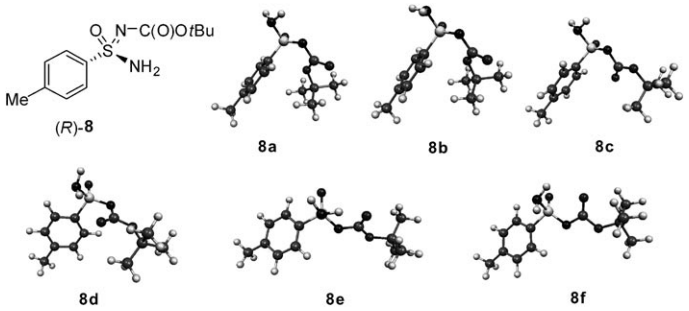

Entry	Conformer	ZPE+MP2/6-311++G**//MP2/6-31+G*[a] E_{tot}	E_{rel}	W[b]
1	**8a**	−1198.576958	0.000	0.7526
2	**8b**	−1198.575065	1.188	0.1012
3	**8c**	−1198.574368	1.625	0.0484
4	**8d**	−1198.574347	1.638	0.0473
5	**8e**	−1198.574169	1.750	0.0392
6	**8f**	−1198.572997	2.486	0.0113

[a] Zero-point energy calculated at the MP2/6-31G* level of theory. [b] *w* is the Boltzmann factor calculated at 298 K.

Table 2. Structures of the five stable conformers found for (*R*)-**9** (**9a–f**) optimized at the MP2/6-31+G* level and their total (in Hartrees) and relative energies (in kcal mol^{-1}) including the ZPE correction.

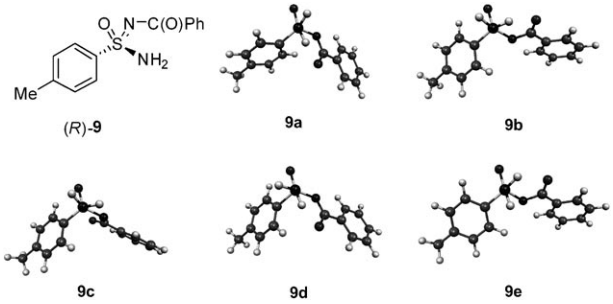

Entry	Conformer	ZPE+MP2/6-311++G**//MP2/6-31+G*[a] E_{tot}	E_{rel}	W[b]
1	**9a**	−1197.152699	0.000	0.6423
2	**9b**	−1197.151517	0.742	0.1836
3	**9c**	−1197.150607	1.313	0.0700
4	**9d**	−1197.150605	1.314	0.0698
5	**9e**	−1197.149935	1.734	0.0343

[a] Zero point energy calculated at the MP2/6-31G* level of theory. [b] *w* is the Boltzmann factor calculated at 298 K.

$$\Delta\varepsilon = \sum_{i=1}^{N} w_i \cdot \Delta\varepsilon_i$$

with

$$w_i = [\exp(-E_i/RT)]/[\sum_{j=1}^{N} \exp(-E_j/RT)]$$

where w_i and E_i are the Boltzmann factor and the energy of the ith local minimum, respectively.

The six most stable conformers (**8a–f**) were included in the calculation of the CD curve of **8**. The leading electronic configurations and calculated rotational strengths for the lowest excited states of the most stable conformer **8a** (Boltzmann factor $w=0.75$) which dominates the shape of the averaged CD spectrum (Figure 2a) are listed in Table 3. The highest occupied and lowest unoccupied Kohn–Sham orbitals of **8a** are shown in Figure 1.

According to the TDDFT calculations the first calculated Cotton effect in the averaged CD spectrum is positive and has a maximum around 246 nm. We assign this Cotton effect to the negative experimental one with a minimum at 231 nm (see Figure 3b). It is mainly due to π+n → π* and π+n+σ → π* transitions from the HOMO (Ψ72) and HOMO−1 (Ψ71) to the LUMO (Ψ73) which occur between 249 and 237 nm for the most stable conformer. The next calculated Cotton effect is more intense and has a maximum around 193 nm and a shoulder at 210 nm. The main contributions to this band come from n+σ → π* transitions from HOMO−5 (Ψ67) to LUMO+1 (Ψ74), π+n → π* transitions from HOMO−3 (Ψ69) to LUMO+1 (Ψ74), and π+n → Ry* transitions from HOMO−3 (Ψ69) and HOMO−2 (Ψ70) to LUMO+2 (Ψ75). This band is positive and we correlate it with the negative one observed at 197 nm. The two calculated Cotton effects are separated by a minimum around 225 nm which has its experimental counterpart in the maximum at 216 nm in the recorded spectrum. As can be seen from Figures 2a and b the shape of the

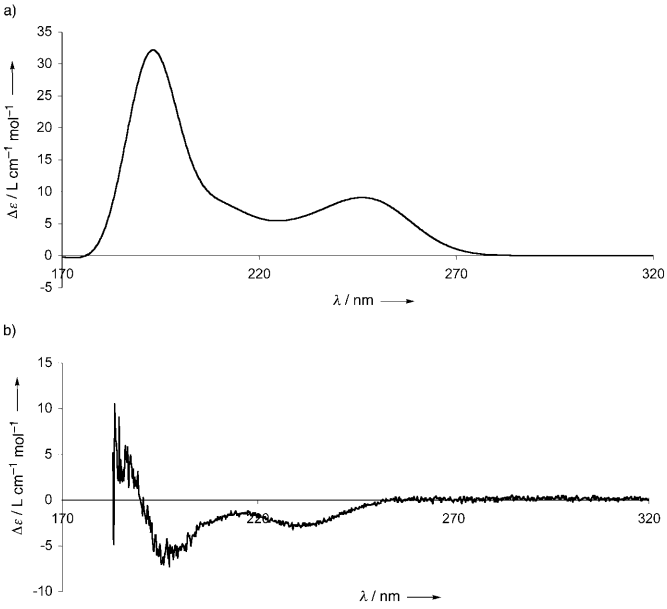

Figure 2. a) Averaged calculated CD spectrum of (*R*)-**8**. b) Experimental CD spectrum of **8**.

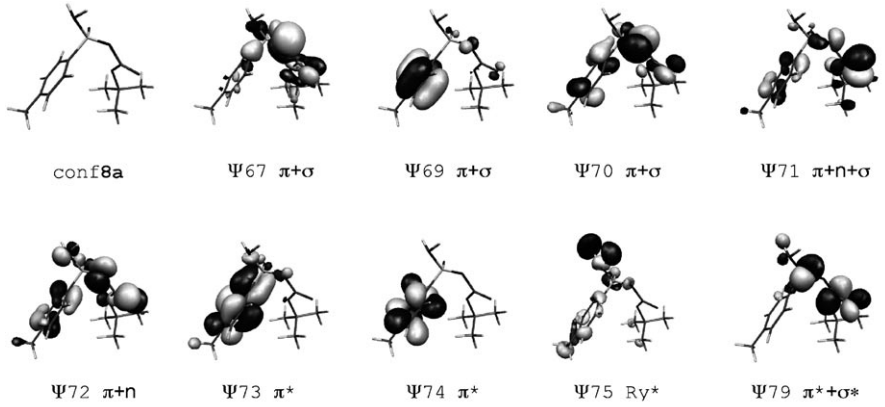

Figure 1. Kohn–Sham orbitals of the most stable conformer **8a**, Ψ72: HOMO, Ψ73: LUMO.

Table 3. Electronic configurations and calculated rotational strengths for the lowest excited states of the most stable conformer **8a** (Boltzmann factor $w=0.75$).

Entry	λ [nm]	Transition	Type	Angle[a] Θ [°]	Rotational strength[b]
1	249.3	HOMO → LUMO	π+n → π*	68.2	20.7
2	237.0	HOMO−1 → LUMO	π+n+σ → π*	71.4	7.4
3	224.1	HOMO → LUMO+1	π+n → π*	80.1	3.4
		HOMO−1 → LUMO+1	π+n+σ → π*		
4	216.8	HOMO−1 → LUMO+1	π+n+σ → π*	60.7	4.4
		HOMO−2 → LUMO+1	π+n → π*		
5	206.5	HOMO−1 → LUMO+6	π+n+σ → π*+ σ*	34.4	17.1
		HOMO → LUMO+6	π+n → π*+ σ*		
6	193.0	HOMO−5 → LUMO+1	n+σ → π*	65.6	55.7
7	191.9	HOMO−3 → LUMO+2	π+n → Ry*	25.1	34.2
8	190.1	HOMO−2 → LUMO+2	π+n → Ry*	86.2	25.1
		HOMO−3 → LUMO+1	π+n → π*		
9	189.3	HOMO−2 → LUMO+2	π+n → Ry*	85.5	25.9

[a] Θ is the angle between the electric and the magnetic transition moments. [b] Rotational strength is given in 10^{-40} erg esu cm Gauss^{-1}.

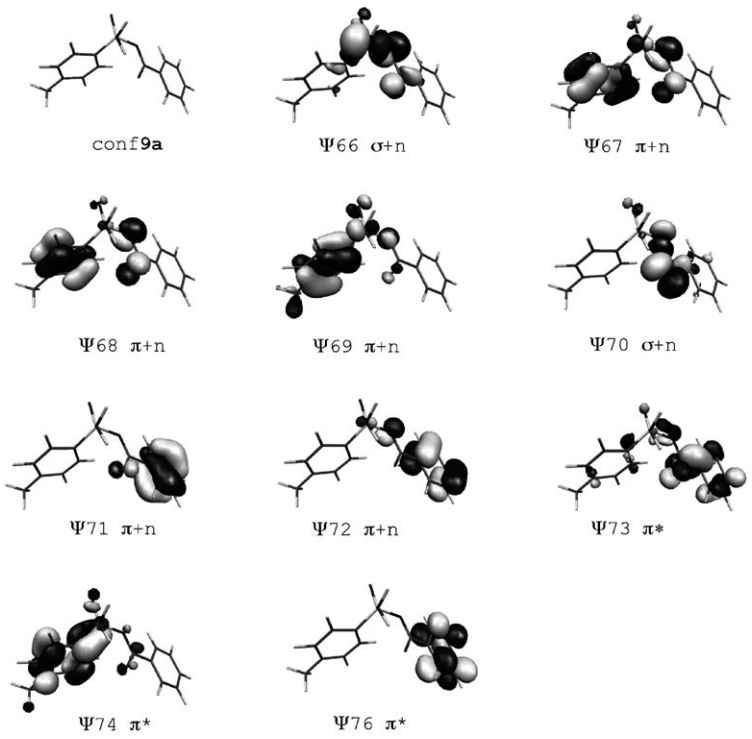

Figure 3. Kohn–Sham orbitals of the most stable conformer **9a**, Ψ72: HOMO, Ψ73: LUMO.

calculated CD spectrum closely resembles the mirror image of the measured spectrum. Since the CD spectrum was calculated for the *R* enantiomer, we conclude that the absolute configuration of sulfonimidamide **8** is most likely *S*.

The calculated and recorded CD spectra of **9** are presented in Figure 4a and b, respectively. All five stable conformers found for **9** (**9a**–**e**) were included in the calculation of the CD curve of **9**. The leading electronic configurations and calculated rotational strengths for the lowest excited states of the most stable conformer **9a** (Boltzmann factor $w=0.64$) which determine the shape of the averaged theoretical CD spectrum (Figure 4a) are listed in Table 4. The highest occupied and lowest unoccupied Kohn–Sham orbitals of **9a** are shown in Figure 3.

According to the TDDFT calculations the first calculated Cotton effect in the averaged CD spectrum is positive and has a maximum around 251 nm and a tail in the long wavelength region. We assign this Cotton effect to the negative experimental one at around 247 nm (see Figure 4b). It is mainly due to $\pi+n \rightarrow \pi^*$ transitions from the HOMO (Ψ72) to the LUMO (Ψ73) which occur in a region between 262 and 249 nm for the most stable conformer. The next calculated Cotton effect occurs at about 226 nm and it is due to several $\pi+n \rightarrow \pi^*$ transitions (HOMO−5 (Ψ67) to LUMO (Ψ73), HOMO−4 (Ψ68) to LUMO (Ψ73) and HOMO−3 (Ψ69) to LUMO+1 (Ψ74)). It is negative and we correlate it with the positive one observed at 228 nm. The third calculated Cotton effect with a maximum at 202 nm is also negative and corresponds most likely to the positive band at 205 nm in the recorded spectrum. The main contribution to this band is given by a $\pi+n \rightarrow \pi^*$ transition from HOMO (Ψ72) to LUMO+3 (Ψ76). As it can be seen from Figure 4a and b the shape of the calculated CD spectrum closely reflects the mirror image of the measured spectrum.

Since the CD spectrum was calculated for the *R* enantiomer, we conclude that the absolute configuration of sulfonimidamide **9** is most likely *S*.

The assignment of the absolute configuration of **9** was supported by single crystal X-ray analysis[26] (Figure 5) of sulfonimidoylguanidine derivative **10**.[4] Since the synthesis of **10** starting from **9** does not affect the absolute configuration at sulfur this result confirms that the final step in the synthesis of the sulfonimidamides, that is, the displacement of chloride atom with ammonia, takes place with inversion of configuration at the sulfur atom.

Table 4. Electronic configurations and calculated rotational strengths for the lowest excited states of the most stable conformer **9a** (Boltzmann factor $w=0.64$).

Entry	λ [nm]	Transition	Type	Angle[a] Θ [°]	Rotational strength[b]
1	262.2	HOMO−1 → LUMO	π+n → π*	77.9	13.8
		HOMO → LUMO	π+n → π*		
2	253.0	HOMO−2 → LUMO+1	σ+n → π*	62.5	7.0
3	248.5	HOMO → LUMO	π+n → π*	83.7	44.6
4	239.7	HOMO−3 → LUMO	π+n → π*	74.6	6.8
5	227.9	HOMO−4 → LUMO	π+n → π*	121.8	-56.1
		HOMO−5 → LUMO	π+n → π*		
		HOMO−3 → LUMO+1	π+n → π*		
6	224.4	HOMO−5 → LUMO	π+n → π*	84.3	5.4
7	217.3	HOMO−6 → LUMO	σ+n → π*	176.2	−10.6
8	212.0	HOMO−6 → LUMO+1	σ+n → π*	67.5	6.9
9	202.5	HOMO → LUMO+3	π+n → π*	107.9	−81.1

[a] Θ is the angle between the electric and the magnetic transition moments. [b] Rotational strength is given in 10^{-40} erg esu cm Gauss^{-1}.

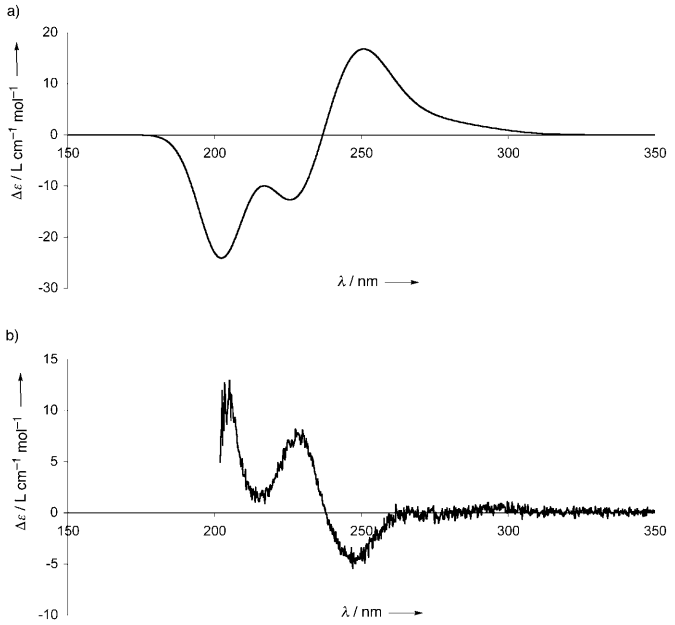

Figure 4. a) Averaged calculated CD spectrum of (*R*)-**9**. b) Experimental CD spectrum of **9**.

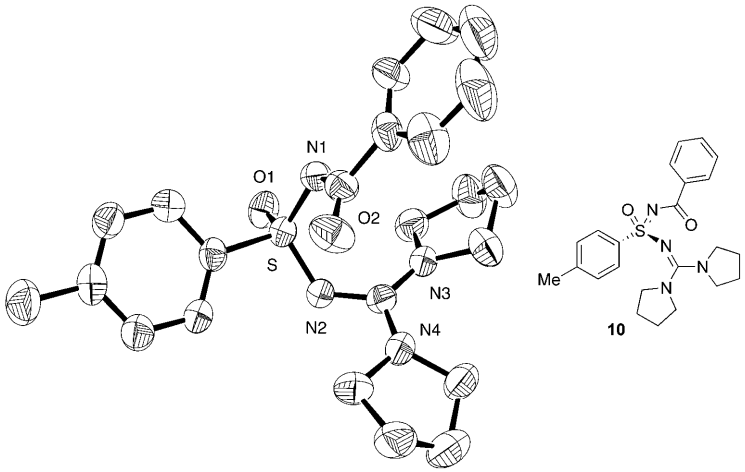

Figure 5. X-ray crystal structure of sulfonimidoylguanidine derivative **10** [Flack parameter $X_{abs} = -0.01(5)$].

Conclusions

We presented four-step syntheses of enantiopure *N*-Bz and *N*-Boc sulfonimidamides with 37 and 29% overall yields, respectively. The approach involves a dynamic resolution of a racemic sulfinic acid sodium salt, and all subsequent steps proceed stereospecifically. The absolute configurations of both products were determined by comparison of measured and calculated CD spectra. The result was confirmed by an X-ray crystal structure determination of a sulfonimidoylguanidine derivative. The enantiopure sulfonimidamides shall now be used as building blocks in newly designed catalysts.[28]

Experimental Section

General methods: All experiments were carried out under an argon atmosphere using standard Schlenk techniques. If necessary, solvents were dried and deoxygenated by standard procedures. NMR spectra were recorded in $CDCl_3$ or [D_6]acetone containing TMS as an internal standard on a Varian Mercury 300 spectrometer (300 and 75 MHz for ^{1}H and ^{13}C NMR spectra, respectively) or a Varian Inova 400 spectrometer (400 and 100 MHz for ^{1}H and ^{13}C NMR spectra, respectively). IR spectra were measured on a Perkin–Elmer Spectrum 100 FT-IR spectrometer with an attached UATR device Diamond/KRS-5 as KBr pellets. MS spectra were recorded on a Finnigan SSQ 7000 using EI as an ionization technique. TLC was carried out on silica gel 60 F_{254} aluminium sheets (Merck) with spot detection under UV light. Optical rotation measurements were conducted at room temperature with a Perkin–Elmer PE 241 polarimeter at a wavelength of 589 nm. Elemental analyses were measured with an Elementar Vario EL. The HPLC measurements were performed on an Agilent system (1100 series) consisting of a degasser G1379 A, a quaternary pump G1311 A, an autosampler G1313A, an oven G1316A and an UV detector G1315B. The CD spectra were measured on a circular dichroism spectrometer (AVIV Model 62DS) at room temperature in acetonitrile.

All starting materials were obtained from commercial suppliers and used without further purification. Menthyl ester **2** was prepared according to the literature procedure.[9]

(*S*)-4-Toluenesulfinamide (3):[9] To a solution of (*S*)-4-toluenesulfinic acid (1*R*,2*S*,4*R*)-menthyl ester (**2**) (6.00 g, 20.4 mmol) in anhydrous THF (100 mL) lithium hexamethyldisilazide (1.06 M in THF, 30.6 mmol, 28.8 mL) was added dropwise over 10 min at −78 °C. The mixture was stirred for 10 min at −78 °C and 1.5 h at room temperature. Then a saturated NH_4Cl solution (in H_2O, 50 mL) was added and stirred for 1 h at room temperature. The reaction mixture was diluted by addition of ethyl acetate (100 mL), the organic layer was separated and the aqueous phase was extracted with ethyl acetate (3×35 mL). The combined organic layers were washed with brine (70 mL), dried ($MgSO_4$), filtered and concentrated under reduced pressure. The product was recrystallized from hexane/ethyl acetate 2:1 (100 mL). (*S*)-4-Toluenesulfinamide (**3**) was isolated as colorless needles (2.75 g, 17.7 mmol, 87%, >99% *ee*). M.p. 115–116 °C [lit.:[10] m.p. 113 °C]; $[\alpha]_D^{20} = +84.5$ ($c = 1.0$ in $CHCl_3$) [lit.:[10] $[\alpha]_D^{20} = +80.2$ ($c = 1.2$ $CHCl_3$)]; ^{1}H NMR (400 MHz, $CDCl_3$): $\delta = 2.41$ (s, 3H, CH_3), 4.35 (s, 2H, NH_2), 7.26–7.32 (m, 2H, Ar-H), 7.59–7.63 ppm (m, 2H, Ar-H); ^{13}C NMR (100 MHz, $CDCl_3$): $\delta = 21.4$ (CH_3), 125.2 (2CH), 129.5 (2CH), 141.3 (C), 143.3 ppm (C); HPLC: $t_r(S) = 20.2$ min, $t_r(R) = 26.2$ min (Chiralpak AD, flow rate 0.7 mL min^{-1}, heptane/*i*PrOH 93:7, $\lambda = 210$ nm, 20 °C).

(*S*)-*tert*-Butyl-(4-tolylsulfinyl)-carbamate (4): To a round bottom Schlenk flask was added (*S*)-4-toluenesulfinamide (**3**) (800 mg, 5.15 mmol) and anhydrous THF (23 mL). After cooling to −78 °C *n*-butyl lithium (1.6 M in hexane, 12.9 mmol, 8.05 mL) was added dropwise over 10 min. The mixture was stirred for 10 min at −78 °C, followed by rapid addition of di-*tert*-butyl dicarbonate (6.18 mmol, 1.35 g). Stirring was continued for 10 min at −78 °C and 3.0 h at room temperature. Then saturated $NaHCO_3$ solution (in H_2O, 23 mL) was added and the reaction mixture was diluted with dichloromethane (45 mL). The organic layer was separated and the aqueous phase was extracted with dichloromethane (5× 15 mL). The combined organic layers were dried ($MgSO_4$), filtered and concentrated under reduced pressure. The product was recrystallized from hexane/ethyl acetate 3:1 (23 mL). (*S*)-*tert*-Butyl-(4-tolylsulfinyl)-carbamate (**4**) was isolated in colorless crystals (828 mg, 3.24 mmol, 63%, >99% *ee*). M.p. 115–116 °C; $[\alpha]_D^{20} = +121$ ($c = 1.0$ in $CHCl_3$); ^{1}H NMR (400 MHz, $CDCl_3$): $\delta = 1.51$ (s, 9H, CH_3), 2.42 (s, 3H, CH_3), 6.66 (s, 1H, NH), 7.31–7.35 (m, 2H, Ar-H), 7.60–7.64 ppm (m, 2H, Ar-H); ^{13}C NMR (100 MHz, $CDCl_3$): $\delta = 21.5$ (CH_3), 28.1 ($3CH_3$), 83.5 (C), 124.6 (2CH), 129.9 (2CH), 140.5 (C), 142.3 (C), 152.3 ppm (CO); IR (KBr): $\tilde{\nu} = 709$, 812, 1063, 1093, 1152, 1238, 1413, 1712, 3116 cm^{-1}; MS (EI, 70 eV): *m*/*z* (%): 256 (1) $[M+H]^+$, 199 (60), 139 (58), 108 (21), 91 (17), 77 (7), 65 (14), 57 (100); elemental analysis calcd (%) for $C_{12}H_{17}NO_3S$: C 56.45, H 6.71, N 5.49; found: C 56.50, H 6.90, N 5.44; HPLC: $t_r(S) = 12.2$ min,

$t_r(R)=17.7$ min (Chiralcel OG, flow rate 1.0 mL min^{-1}, heptane/*i*PrOH 95:5, $\lambda=230$ nm, 20 °C).

(*S*)-*N*-(4-Tolylsulfinyl)-benzamide (5): Same procedure as described for **4**, but use of benzoic anhydride (6.18 mmol, 1.40 g) instead of di-*tert*-butyl dicarbonate. The product was recrystallized from hexane/ethyl acetate (2/1, 30 mL) and (*S*)-*N*-(4-tolylsulfinyl)-benzamide (**5**) was isolated in colorless crystals (814 mg, 3.14 mmol, 61 %, >99 % *ee*). M.p. 121–122 °C; $[\alpha]_D^{20}=+118$ ($c=1.0$ in $CHCl_3$); ^{1}H NMR (300 MHz, $CDCl_3$): $\delta=$ 2.43 (s, 3H, CH_3), 7.31–7.36 (m, 2H, Ar-H), 7.40–7.47 (m, 2H, Ar-H), 7.52–7.59 (m, 1H, Ar-H), 7.61–7.66 (m, 2H, Ar-H), 7.79–7.84 (m, 2H, Ar-H), 8.56 ppm (s, 1H, NH); ^{13}C NMR (75 MHz, $CDCl_3$): $\delta=21.5$ (CH_3), 124.8 (2CH), 127.9 (2CH), 128.8 (2CH), 130.1 (2CH), 131.6 (C), 133.1 (CH), 140.7 (C), 142.6 (C), 167.3 ppm (CO); IR (KBr): $\tilde{\nu}=$ 720, 756, 807, 883, 1069, 1095, 1244, 1387, 1648, 3225 cm^{-1}; MS (EI, 70 eV): *m*/*z* (%): 259 (19) [M^+], 151 (2), 139 (33), 108 (50), 105 (100), 91 (22); elemental analysis calcd (%) for $C_{14}H_{13}NO_2S$: C 64.84, H 5.05, N 5.40; found: C 65.10, H 5.31, N 5.45; HPLC: $t_r(R)=24.9$ min, $t_r(S)=33.0$ min (Chiralcel OD-H, flow rate 1.0 mL min^{-1}, heptane/*i*PrOH 95:5, $\lambda=$ 230 nm, 20 °C).

(*S*)-*N*-*tert*-Butyloxycarbonyl-4-toluenesulfonimidamide (8): A solution of (*S*)-*tert*-Butyl-(4-tolylsulfinyl)-carbamate (**4**) (850 mg, 3.33 mmol) in THF (25 mL) was cooled to 0 °C, and *tert*-butyl hypochlorite (4.33 mmol, 470 mg, 0.489 mL) was then slowly added. The reaction was stirred at 0 °C for 1 h. At 0 °C an aqueous ammonia solution (25 %, 13.3 mL) was added and the reaction mixture was stirred a room temperature overnight. After neutralization of the reaction mixture by addition of a 6 M HCl solution, the organic layer was separated and the aqueous phase was extracted with dichloromethane (4×20 mL). The combined organic layers were dried ($MgSO_4$), filtered and the solvent was removed under reduced pressure. (*S*)-*N*-*tert*-Butyloxycarbonyl-4-toluenesulfonimidamide (**8**) was isolated as a white powder (703 mg, 2.60 mmol, 78 %, >99 % *ee*). M.p. 123–124 °C; $[\alpha]_D^{20}=+14.5$ ($c=1.0$ in $CHCl_3$); ^{1}H NMR (400 MHz, $CDCl_3$): $\delta=1.37$ (s, 9H, CH_3), 2.43 (s, 9H, CH_3), 5.85 (br s, 2H, NH_2), 7.29–7.33 (m, 2H, Ar-H), 7.85–7.89 ppm (m, 2H, Ar-H); ^{13}C NMR (100 MHz, $CDCl_3$): $\delta=21.6$ (CH_3), 28.1 ($3CH_3$), 80.6 (C), 127.1 (2CH), 129.6 (2CH), 137.8 (C), 144.0 (C), 157.1 ppm (CO); IR (KBr): $\tilde{\nu}=$ 697, 739, 799, 849, 952, 1120, 1154, 1238, 1311, 1623, 3280 cm^{-1}; MS (EI, 70 eV): *m*/*z* (%): 271 (1) [$M+H]^+$, 215 (7), 197 (35), 171 (7), 154 (24), 139 (6), 108 (100), 91 (27); elemental analysis calcd (%) for $C_{12}H_{18}N_2O_3S$: C 53.31, H 6.71, N 10.36; found: C 53.32, H 6.66, N 10.40; HPLC: $t_r(R)=17.3$ min, $t_r(S)=22.4$ min (Chiralcel OD, flow rate 1.0 mL min^{-1}, heptane/*i*PrOH 90:10, $\lambda=254$ nm, 20 °C).

(*S*)-*N*-Benzoyl-4-toluenesulfonimidamide (9): Same procedure as for the synthesis of **8**, but use of (*S*)-*N*-(4-tolylsulfinyl)-benzamide (**5**) (800 mg, 3.08 mmol) in THF (50 mL), *tert*-butyl hypochlorite (4.01 mmol, 435 mg, 0.454 mL) and an aqueous ammonia solution (25 %, 12.4 mL). (*S*)-*N*-Benzoyl-4-toluenesulfonimidamide (**9**) was isolated as a white powder (822 mg, 3.00 mmol, 97 %, >99 % *ee*). M.p. 137–139 °C; $[\alpha]_D^{20}=+64.2$ ($c=$ 0.9 in $CHCl_3$); ^{1}H NMR (400 MHz, [D$_6$]acetone): $\delta=2.41$ (s, 3H, CH_3), 7.23 (br s, 2H, NH_2), 7.38–7.43 (m, 4H, Ar-H), 7.48–7.53 (m, 1H, Ar-H), 7.91–7.95 (m, 2H, Ar-H), 8.05–8.09 ppm (m, 2H, Ar-H); ^{13}C NMR (100 MHz, [D$_6$]acetone): $\delta=22.4$ (CH_3), 128.5 (2CH), 129.6 (2CH), 130.7 (2CH), 131.1 (2CH), 133.4 (CH), 138.2 (C), 141.6 (C), 145.2 (C), 173.4 ppm (CO); IR (KBr): $\tilde{\nu}=$ 716, 806, 838, 980, 1152, 1217, 1298, 1324, 1449, 1573, 1600, 3288 cm^{-1}; MS (EI, 70 eV): *m*/*z* (%): 275 (1) [$M+H]^+$, 197 (4), 154 (1), 139 (4), 108 (100), 91 (17); elemental analysis calcd (%) for $C_{14}H_{14}N_2O_2S$: C 61.29, H 5.14, N 10.21; found: C 61.31, H 5.22, N 9.89; HPLC: $t_r(R)=37.1$ min, $t_r(S)=55.8$ min (Chiralcel OJ, flow rate 0.7 mL min^{-1}, heptane/*i*PrOH 85:15, $\lambda=230$ nm, 20 °C).

Acknowledgements

This work was supported by the Deutsche Forschungsgemeinschaft (DFG, SPP 1179) and the Fonds der Chemischen Industrie.

[1] a) C. Liang, F. R. Peillard, C. Fruit, P. Müller, R. H. Dodd, P. Dauban, *Angew. Chem.* **2006**, *118*, 4757–4760; *Angew. Chem. Int. Ed.* **2006**, *45*, 4641–4644; b) C. Liang, F. Collet, F. R. Peillard, P. Müller, R. H. Dodd, P. Dauban, *J. Am. Chem. Soc.* **2008**, *130*, 343–350.
[2] a) D. Leca, A. Toussaint, C. Mareau, L. Fensterbank, E. Lacôte, M. Malacria, *Org. Lett.* **2004**, *6*, 3573–3575; b) P. H. Di Chenna, F. Robert-Peillard, P. Dauban, R. H. Dodd, *Org. Lett.* **2004**, *6*, 4503–4505; c) C. Fruit, F. Robert-Peillard, G. Bernardinelli, P. Müller, R. H. Dodd, P. Dauban, *Tetrahedron: Asymmetry* **2005**, *16*, 3484–3487.
[3] F. Collet, R. H. Dodd, P. Dauban, *Org. Lett.* **2008**, *10*, 5473–5476.
[4] C. Worch, C. Bolm, *Synthesis* **2007**, 1355–1358.
[5] C. Worch, C. Bolm, *Synthesis* **2008**, 739–742.
[6] S. Azzaro, L. Fensterbank, E. Lacôte, M. Malacria, *Synlett* **2008**, 2253–2256.
[7] For early studies of sulfonimidamides, see: a) E. S. Levchenko, N. Y. Derkach, A. V. Kirsanov, *Zh. Obshch. Khim.* **1962**, *32*, 1208–1212; b) C. R. Johnson, E. U. Jonsson, C. C. Bacon, *J. Org. Chem.* **1979**, *44*, 2055–2061; c) E. U. Jonsson, C. C. Bacon, C. R. Johnson, *J. Am. Chem. Soc.* **1971**, *93*, 5306–5308; d) E. U. Jonsson, C. R. Johnson, *J. Am. Chem. Soc.* **1971**, *93*, 5308–5309; e) J. E. Toth, J. Ray, J. Deeter, *J. Org. Chem.* **1993**, *58*, 3469–3472.
[8] For interesting bioactive sulfonimidamide derivatives, see: a) C. L. Hillemann (Du Pont), US Patent 4666506, **1987**; b) J. E. Toth, G. B. Grindey, W. J. Ehlhardt, J. E. Ray, G. B. Boder, J. R. Bewley, K. K. Klingerman, S. B. Gates, S. M. Rinzel, R. M. Schultz, L. C. Weir, J. F. Worzalla, *J. Med. Chem.* **1997**, *40*, 1018–1025; c) B. E. Cathers, J. V. Schloss, *Bioorg. Med. Chem. Lett.* **1999**, *9*, 1527–1532.
[9] a) L. B. Krasnova, A. K. Yudin, *J. Org. Chem.* **2004**, *69*, 2584–2587; b) G. Solladié, *Synthesis* **1981**, 185–196; c) C. Mioskowski, G. Solladié, *Tetrahedron* **1980**, *36*, 227–236.
[10] F. A. Davis, Y. Zhang, Y. Andemichael, T. Fang, D. L. Fanelli, H. Zhang, *J. Org. Chem.* **1999**, *64*, 1403–1406.
[11] B. J. Backes, D. R. Dragoli, J. A. Ellman, *J. Org. Chem.* **1999**, *64*, 5471–5478.
[12] M. J. Mintz, C. Walling, *Org. Synth.* **1973**, *5*, 184–187.
[13] For related sulfinamides it was shown that the oxidative chlorination using *tert*-butyl hypochlorite proceeds with retention of configuration. M. Reggelin, B. Junker, *Chem. Eur. J.* **2001**, *7*, 1232–1239.
[14] For oxidative chlorinations of sulfinamides with *N*-chlorosuccinimide, where the stereochemical path remained undetermined, see: O. Garcia Mancheno, C. Bolm, *Beilstein J. Org. Chem.* **2007**, *3*, 25.
[15] The Monte–Carlo method used in our calculations is based on a standard simulated annealing algorithm with a temperature ramp of $T=T_f-\Delta T(1-I/I_{max})^3$, where $\Delta T=T_f-T_i$. In these equations T_i, T_f and T are the initial, final and the current temperature. I and I_{max} represent the current step number and the maximal number of steps. I_{max} depends on the number of flexible centres of the studied molecule as well as the number of increments in the rotation. Finally, the new conformation is weighted via the Boltzmann criteria.
[16] Spartan, Version 02, Wavefunction, Inc. 18401 Von Karman Ave., Suite 370, Irvine, CA 92612.
[17] T. A. Halgren, *J. Comput. Chem.* **1996**, *17*, 490–519.
[18] Gaussian 03, Revision D.02, M. J. Frisch, G. W. Trucks, H. B. Schlegel, G. E. Scuseria, M. A. Robb, J. R. Cheeseman, J. A. Montgomery, Jr., T. Vreven, K. N. Kudin, J. C. Burant, J. M. Millam, S. S. Iyengar, J. Tomasi, V. Barone, B. Mennucci, M. Cossi, G. Scalmani, N. Rega, G. A. Petersson, H. Nakatsuji, M. Hada, M. Ehara, K. Toyota, R. Fukuda, J. Hasegawa, M. Ishida, T. Nakajima, Y. Honda, O. Kitao, H. Nakai, M. Klene, X. Li, J. E. Knox, H. P. Hratchian, J. B. Cross, V. Bakken, C. Adamo, J. Jaramillo, R. Gomperts, R. E. Stratmann, O. Yazyev, A. J. Austin, R. Cammi, C. Pomelli, J. W. Ochterski, P. Y. Ayala, K. Morokuma, G. A. Voth, P. Salvador, J. J. Dannenberg, V. G. Zakrzewski, S. Dapprich, A. D. Daniels, M. C. Strain, O. Farkas, D. K. Malick, A. D. Rabuck, K. Raghavachari, J. B. Foresman, J. V. Ortiz, Q. Cui, A. G. Baboul, S. Clifford, J. Cioslowski, B. B. Stefanov, G. Liu, A. Liashenko, P. Piskorz, I. Komaro-

mi, R. L. Martin, D. J. Fox, T. Keith, M. A. Al-Laham, C. Y. Peng, A. Nanayakkara, M. Challacombe, P. M. W. Gill, B. Johnson, W. Chen, M. W. Wong, C. Gonzalez, J. A. Pople, Gaussian, Inc., Wallingford CT, **2004**.

[19] Graphics obtained by MOLEKEL 4.3, P. Flükiger, H. P. Lüthi, S. Portmann, J. Weber, Swiss Center for Scientific Computing, Manno, **2000–2002**.

[20] R. Bauernschmitt, R. Ahlrichs, *Chem. Phys. Lett.* **1996**, *256*, 454–464.

[21] a) C. Lee, W. Yang, R. G. Parr, *Phys. Rev. B* **1988**, *37*, 785–789; b) B. Miehlich, A. Savin, H. Stoll, H. Preuss, *Chem. Phys. Lett.* **1989**, *157*, 200–206; c) A. D. Becke, *J. Chem. Phys.* **1993**, *98*, 5648–5652.

[22] A. Moscowitz in *Modern Quantum Chemistry, Vol. 3* (Ed.: O. Sinanoglu), Academic Press, New York, **1965**, pp. 31–44.

[23] J. A. Schellman, *Chem. Rev.* **1975**, *75*, 323–331.

[24] A. Brown, C. M. Kemp, S. F. Mason, *J. Chem. Soc. A* **1971**, 751–755.

[25] R. W. Woody, private communication.

[26] Suitable crystals were obtained from ethyl acetate. The compound ($C_{23}H_{28}N_4O_2S$) crystallizes in orthorhombic space group $P2_12_12_1$ (19) with cell constants $a=8.643(2)$, $b=13.364(15)$, and $c=19.173(4)$ Å. At a molecular weight of 424.57, $Z=4$ and a cell volume of 2215(3) Å^3 the density and the linear absorption coefficients are 1.273 g cm^{-3} and 1.509 mm^{-1}, respectively. No absorption correction. Diffraction data were collected at 298 K on an Enraf Nonius CAD4 diffractometer employing $Cu_{K\alpha}$ radiation ($\lambda=1.54179$ Å). 4565 reflections were collected in the range $-10\le h\le 10$, $-16\le k\le 14$, and $-23\le l\le 23$ ($\theta_{max}=67.9°$), merged to give 3959 independent reflections ($R_{int}=0.02(4)$). The structure was solved by direct methods as implemented in the XTAL3.7 package of crystallographic routines[27] employing GENSIN[27] to generate structure-invariant relationships and GENTAN[27] for the general tangent phasing procedure. 3783 observed reflections ($I>2\sigma(I)$) were included in a full-matrix least squares refinement of 271 parameters converging at $R(R_w)=0.07(0.09$; $w=1/\sigma^2(F))$, and a residual electron density of $-0.90/+0.53$ e Å^{-3}. Most of the hydrogen atoms were located and the rest were calculated in idealized positions. No refinement of hydrogen parameters. Flack parameter $X_{abs}=-0.01(5)$ for the structure shown in Figure 5. CCDC 734215 contains the supplementary crystallographic data for this paper. These data can be obtained free of charge from The Cambridge Crystallographic Data Centre via www.ccdc.cam.ac.uk/data_request/cif.

[27] a) XTAL3.7 System, S. R. Hall, D. J. du Boulay, R. Olthof-Hazekamp, University of Western Australia, Perth, **2000**; b) GENSIN, XTAL3.7 System, V. Subramanian, S. R. Hall, University of Western Australia, Perth, **2000**; c) GENTAN, XTAL3.7 System, S. R. Hall, S. R. Hall, D. J. du Boulay, R. Olthof-Hazekamp, University of Western Australia, Perth, **2000**.

[28] For initial investigations along these lines, see: C. Worch, C. Bolm, *Synlett* **2009**, 2425–2428.

Received: June 22, 2009
Revised: September 10, 2009
Published online: November 24, 2009

